Characterisation of Two Wood-Waste and Coffee Bean Husk Biochars for the Removal of Micropollutants from Water

Thessa Van Limbergen[1,2†], Inez Henriette Roegiers[3†], Robin Bonné[2,4], Federica Mare[1], Tom Haeldermans[5], Bjorn Joos[6,7,8], Olivier Nouwen[1], Jean V. Manca[2], Jaco Vangronsveld[1,9] and Sofie Thijs[1]*

[1]Department of Biology, Environmental Microbiology, Centre for Environmental Sciences, Faculty of Sciences, Hasselt University, Diepenbeek, Belgium, [2]X-LAB, Department of Physics, Faculty of Sciences, Hasselt University, Diepenbeek, Belgium, [3]Center for Microbial Ecology and Technology, Faculty of Bioscience Engineering, Ghent University, Ghent, Belgium, [4]Department of Bioscience, Center for Electromicrobiology, Aarhus University, Aarhus, Denmark, [5]Research Group of Analytical and Applied Chemistry, IMO, Hasselt University, Diepenbeek, Belgium, [6]Institute for Materials Research (imo-imomec), DESINe Team, Hasselt University, Diepenbeek, Belgium, [7]Imec, Division Imomec, Diepenbeek, Belgium, [8]EnergyVille, Genk, Belgium, [9]Department of Plant Physiology and Biophysics, Institute of Biological Sciences, Maria Curie-Skłodowska University, Lublin, Poland

The inclusion of bioaugmented low-cost biochar in current wastewater treatment technologies is a promising way to enhance the removal and degradation of emerging contaminants. In this paper, the properties of two wood waste biochars (wood waste mix - AB, and date palm fiber wood - PDF), and coffee bean husks (COF), produced at four temperatures (350, 450, 500, 550°C) were compared, and investigated in the presence of *Geobacter sulfurreducens* or a mixed freshwater stream bacterial culture to understand their potential for the adsorption and biotransformation of two types of pesticides (thiacloprid, pirimicarb), and two pharmaceuticals (ibuprofen, diclofenac). Biochar yield was similar for all three biochars and ranged between 30 and 35%. The ash content of PDF and COF was significantly higher than AB. pH and electrical conductivity (EC) were initially high for COF (pH: 7.4–8; EC: 3–4.27 mS/cm) and PDF (pH: 7.7–10.1; EC: 4–6.24 mS/cm) after 24 h, but stabilized at neutral pH and <0.5 mS/cm EC after additional washes. COF and AB did not leach high concentrations of chloride (<10 mg/L), nitrate (<1 mg/L), nor sulphate (<76 mg/L), this in contrast to date palm fiber wood (PDF) with 1760 mg/L Cl⁻ (550°C), and 846 mg/L sulphate (350°C). Lower pyrolysis temperatures reduced leachable anions. The biochars were highly (ultra)microporous with little meso- and macroporosity. The adsorption experiments showed that AB and COF biochars were both suited to sorb more than 90% of the initially spiked 10 ppm pirimicarb, AB removed 50.2% of the initial diclofenac concentration compared to only 5% for the no-biochar control, and both biochars could remove about 55% of the initially spiked thiacloprid, and 40% of the ibuprofen. In the presence of a mixed culture, on average 30% more thiacloprid and ibuprofen was removed from the supernatant by AB and COF than the sterile control. This work shows that selected wood-waste feedstocks and low pyrolysis temperature can produce environmentally-safe biochars that have suitable characteristics to sorb emergent

pollutants from water. These materials could be further studied in multi-pollution sorption/ competition experiments, and in larger environmental wastewater treatment systems.

1 INTRODUCTION

The presence of emerging contaminants in wastewater such as pharmaceuticals and pesticides represent a significant problem worldwide. Only until recently, we were able to quantify the presence of these micropollutants in water streams, and this means that regulation is inexistent or still in progress, and their removal contains still large knowledge gaps. The levels found in finished drinking water vary substantially per component, and per country, but levels up to 3 ng/L and 35 ng/L of ibuprofen (Patel et al., 2019) and diclofenac (Żur et al., 2021), respectively, have been measured. The global pesticide usage is estimated at 3.5 million tons/per year (Sharma et al., 2019), and a significant portion of it ends up as rest products in surface-and groundwater (de Souza et al., 2020).

Pharmaceuticals and pesticides are not typically broken down in current wastewater treatment processes, because of their low concentrations and their molecular structures which are not easily metabolized by bacteria (Manoli et al., 2019). Advanced installations to remove pesticides from wastewater (e.g., Sentinel; Allman and Co., Ltd. Birdham, United Kingdom), comprise sand or membrane filtration, followed by activated carbon filtration, and/or advanced oxidation processes. These methods are more effective, though not always reaching 100% completeness in removing the pollutants, and they entail high installation and operational costs (Rizzo et al., 2015). In addition, the regeneration of the activated carbon is expensive, energy intensive and depends on a non-durable industry. Therefore, there is a need for creating more cost-efficient methods and/or improving on current wastewater treatment systems, such as constructed wetlands.

An emerging technology is the incorporation of bioelectrochemical systems (BES) and electroactive bacteria (EAB) in constructed wetlands, as has been shown to hold promise not only for the removal of high BOD and COD wastewater (Aguirre-Sierra et al., 2016), but also for emerging contaminants from water (Kozyatnyk et al., 2021). In BES, electroactive bacteria couple the oxidation of pollutants to the reduction of an electrode that functions as an anode in an electrochemical cell (Liu et al., 2009; Jain and He, 2018). A lot of materials have been used as anode material, such as carbon cloth, graphite felt and carbon mesh, chosen for their low electrical resistance, high conductivity, chemical stability and large surface area for the bacteria to attach on (Logan et al., 2007). In constructed wetlands, the surface area in the anodic compartment can be expanded even more with the addition of granular activated carbon (GAC) to the anodic compartment thereby increasing the attachment of bacteria, showing more current being produced (Wang et al., 2017), and higher

biodegradation rates than non-adsorbing or non-conductive media (e.g., sand) (Aguirre-Sierra et al., 2016). A more sustainable solution to this would be the use of biochar, recycled and produced from wood waste-material as alternative to the activated carbon, that can function as both a bacterial substrate and an adsorbing agent.

Biochar is a carbon-rich solid material produced by thermal decomposition of diverse waste biomass species under oxygen-limited conditions (pyrolysis) (Tomczyk et al., 2020). The main properties that make biochar an interesting possible addition to a BES are: 1) the porous structure, which can immobilize the contaminants and therefore decreases their bioavailability and ecotoxicity, 2) the ability to act as an electron shuttle and donate and receive electrons from electroactive bacteria (Prévoteau et al., 2016; Yuan et al., 2017), 3) the ability to act as a substrate for electroactive bacteria (Prévoteau et al., 2016) and plants. In 2014, Chen et al. showed that biochar can facilitate interspecies electron transfer. Also, when compared to GACs, the anaerobic metabolism of the biofilm is higher (Chen et al., 2014). Biochar thus has many environmental benefits and comes at a very low production cost. It can become an improvement in BES for large-scale wastewater treatment operations (Aguirre-Sierra et al., 2016; Tejedor-Sanz et al., 2017, 2018). Biochar has a longer lifetime compared to GACs, and wood-derived biochar has already been studied as a possible replacement for GACs in contaminant removal applications (Yuan et al., 2017).

Before large-scale additions of biochar in BES are possible, we need to understand the differences and properties of biochars pyrolysed at different temperatures on pesticide and pharmaceutical removal. For example, what is the influence of temperature on pH, leaching of nitrate, nitrite, sulfate from biochars, and their efficacy in adsorbing contaminants. Therefore, the objective of this study was to compare the properties of three waste-material biochars after pyrolization at different temperatures. Two pesticides (thiacloprid, pirimicarb) and two pharmaceuticals (ibuprofen, diclofenac) were chosen because of their low biodegradability, and high prevalence in the wastewater. Both thiacloprid and pirimicarb are used as neonicotinoid insecticides, which act on the central nervous system of insects by inhibiting acetylcholinesterase activity. Structurally they are different, as pirimicarb is a member of the dimethylcarbamate group (Soloneski and Larramendy, 2015), and thiacloprid is a chloropyridinyl-cyanamide compound (Pang et al., 2020). Additionally, the effect of biochar on pollutant removal in the presence of a mixed bacterial culture or pure culture of G. sulfurreducens was studied, as well as the colonization potential of the bacteria on the biochars.

2 MATERIAL AND METHODS

2.1 Biochar Material and Pyrolysis

The biochars used in this research were fibers from date palm (PDF) (*Phoenix dactylifera*), husks of coffee beans (COF) and wood waste (AB). The wood waste was kindly provided by Gielen NV (Genk, Belgium) and is a mix of category A wood waste (untreated wood waste) and category B wood waste (non-contaminated, treated wood waste). Examples of type A wood are pallets and fruit cases, type B wood is for example multiplex wood, MDF or painted wood. All materials were ground to a particle size of <1 cm with a Retsch SM100 grinder. For the pyrolysis, a custom-made reactor was used as described before (Vanreppelen et al., 2014). The reactor was heated in a Nabertherm oven and controlled with an FGH100 controller. The materials were pyrolysed at four temperatures (350, 450, 500 and 550°C) with a heating-up rate of 15°C/min and a residence time of 30 min. An Archimedes' screw rotated the biomass around with a speed of 400 rpm and nitrogen gas (N_2) was supplied with a speed of 2×70 ml/min. Further treatment of the biochars consisted of baking overnight at 100°C for the removal of surface oils, followed by a washing step to remove additional soluble oils and surface precipitates such as PAH's and lastly, they were once more dried overnight at 100°C. The biochars were ground and sieved to a size range of 0.85–1.00 mm.

The granular activated carbon used was Cyclecarb 301®, kindly provided by Chemviron, Teluy, Belgium. It has a particle size of 1–2 mm, bed density of 450 kg/m³, N_2 BET surface area of 900 m²/g and moisture content of 2% w/w.

2.2 Biochar Characterization

2.2.1 pH, Wet Conductivity and Leaching in Solution

The biochars were brought into suspension in a 1:20 ratio with Milli-Q water. After 24 h of shaking, the biochars were filtered with Rotilabo A14 ashless filters (Carl Roth, Karlsruhe, Germany). The pH, conductivity and leaching of anions were determined respectively with a Knick pH meter 764 (Knick International, Berlin, Germany), a LF537 conductivity meter (WTW, Berlin, Germany) and a DX120 ion chromatograph (IC) (ThermoFisher Scientific, Waltham, United States). The residues were dried at 105°C and then suspended as described above for measurements after 48 and 72 h. Samples were compared to Milli-Q as control. Values were compared against the norms set for surface water quality in Flanders, Belgium (VLAREM II: https://navigator.emis.vito.be/mijn-navigator?woId=10071).

2.2.2 Porosity and Pore Structure

The porosity of the biochars was determined by means of N_2 and CO_2 physisorption at 77.35 K (cryogenic nitrogen) and 273.15 K (ice-water bath) respectively with a Micromeritics Tristar II 3020 (Norcross, Georgia, United States). Residual moisture and surface contaminants were removed under nitrogen flushing at an elevated temperature of 150°C overnight. The specific surface area S_{BET} was calculated by means of the Brunauer–Emmett–Teller (BET) theory by the selection of the appropriate relative pressure range, suggested by Rouquerol for microporous materials (Brunauer et al., 1938; Rouquerol et al., 2007). The specific surface area correlated to the micropores, i.e., Sw < 2, and the meso- and macropores, i.e., S2<w < 300, were estimated with the thickness-plot (t-plot) method and Barrett–Joyner–Halenda theory (BJH) respectively (Barrett et al., 1951; Lippens and Boer, 1965). The BJH theory was also used to calculate the pore size distribution of the wider micropores (width >1 nm), and the meso- and macropores.

2.2.3 Moisture Content

The moisture content was determined according to the standard method ASTM D286-04. 1–2 g of biochar were heated in porcelain crucibles at a temperature of 150°C for 3 hours. The samples were then cooled in a desiccator to room temperature. The percentage of moisture content was determined by comparison (**Eq. 1**):

$$\% \text{ moisture content} = \frac{C - D}{C - B} \times 100\% \qquad (1)$$

with B the weight of the (empty) porcelain crucible, C the weight of the porcelain crucible with the biochar before drying, and D the weight of the porcelain crucible with the biochar after drying.

2.2.4 Ash Content

The ash content was determined according to the standard method of ASTM, reference ASTM D2866-94. A quantity of biochar sample was dried for 3 h at 150°C in a porcelain crucible. Sufficient sample was weighed and ignited at 650 ± 25°C for 3–16 h. After ashing, the samples were cooled in a desiccator and weighed. The ash content was determined by comparison (**Eq. 2**):

$$\% \text{ ash content} = \frac{D - B}{C - B} \times 100\% \qquad (2)$$

with B the weight of the (empty) crucible, C the weight of the crucible and the dried sample, and D the weight of the crucible after ignition.

2.2.5 Yield

The biochar yield was expressed as the ratio of the amount of biochar formed to the initial biomass (30 g) as shown in comparison (**Eq. 3**).

$$\% \text{ yield} = \frac{A}{B} \times 100\% \qquad (3)$$

with A the amount of biochar after pyrolysis (g) and B the initial biomass (g).

2.3 Bacteria and Culture Conditions

Geobacter sulfurreducens strain 12,127 was obtained from DSMZ (Braunschweig, Germany). A mixed bacterial culture was established by adding some scoops of sediment from the Stiemerbeek, a stream in Diepenbeek (Belgium) to a sterile anaerobic flask with fresh water medium (Borjas et al., 2017). The mixed culture was incubated at 30°C in the dark for 5 days and then a 1:10 transfer was performed to a new flask, incubated

for 1 week. This was the stock solution to use at the start of experiments.

For culturing, 20 mM Na-acetate ($NaC_2H_3O_2$, 1.64 g/L) and 40 mM Na-fumarate ($C_4H_2Na_2O_4$, 6.40 g/L) was added as electron donor and acceptor, respectively. Medium was prepared by combining all components mentioned above and transferred to 12 ml tubes for anaerobic culturing (Chemglass Life Sciences, Vineland, United States). Medium was flushed for 15 min with N_2, headspace was flushed for 5 min with N_2 and the tube closed with a tight butyl seal (Rubber B.V., Hilversum, Netherlands). Afterwards, 2 ml of CO_2 was injected with a sterile needle in the headspace and N_2 was added to reach 1.4 bars over-pressure. The final headspace gas composition was approximately 80:20 N_2/CO_2. Tubes were autoclaved for 15 min at 121°C (Liquid A program, Tuttnauer, Breda, Netherlands). After autoclaving, 1 ml of pure or mixed bacterial culture was injected and the tubes were placed in a dark room at 30°C. Routinely, bacteria were also cultured in 60 ml glass vials (548-0,609, VWR, Radnor, United States), in the same medium as described above. Pesticides or pharmaceuticals were injected under sterile conditions using a Hamilton syringe (VWR, Radnor, United States).

2.4 Pesticides and Pharmaceutical Stocks, and HPLC Reagents

Pesticides were spiked in the media from concentrated stock solutions, to reach final concentrations of 10 mg/L. A stock of 10 g/L thiacloprid (PESTANAL®, 37,905, analytical standard, Sigma-Aldrich, St. Louis, United States) was dissolved in DMSO. A pirimicarb (PESTANAL®, 45,627, analytical standard, Sigma-Aldrich, St. Louis, United States) solution of 1 g/L was made in Milli-Q water, filter sterilized (45 μm, VWR, Radnor, United States) and flushed with N_2 gas for 10 min. Sodium-diclofenac (≥98%) was purchased from Acros Organics (Geel, Belgium) and a stock solution of 10 g/L was made in DMSO. Sodium-Ibuprofen (≥98%) was purchased from VWR (Leuven, Belgium) and a stock solution of 1,000 mg/L was made in Mili-Q water. Methanol Chromasolv™ ≥99.9% pure, and Acetonitrile HiPerSolv ChromaNorm® ≥99.9% pure were purchased from VWR, Belgium for pollutant extractions and HPLC.

2.5 Anaerobic Degradation of Pharmaceuticals by Growing Cultures
2.5.1 Without Biochar or Activated Carbon
One ml of growing cells of *G. sulfurreducens* and mixed culture cells (log-growth phase determined spectrophotometrically at OD_{600}), were transferred to 10 ml of sterile FWM medium in Hungate tubes, supplemented with 10 mg/L of either pharmaceutical or pesticide. The applied concentration of pollutants was higher than environmentally relevant, in order to amplify the possible metabolizing properties of the bacteria—a similar approach is used in the screening of xenobiotics metabolizing strains. The test conditions of pesticide degradation were in medium containing both 20 mM acetate

and 40 mM fumarate, 20 mM acetate only, or 40 mM fumarate only. All conditions were tested in threefold and compared to no bacteria controls. Samples were incubated at 30°C for 14 days prior to HPLC analyses and Bradford.

2.5.2 With Biochar or Activated Carbon
Due to the high leaching values of PDF for Cl^- and nitrate, only AB and COF (pyrolyzed at 450°C) were considered for the biochar-amended remediation/degradation experiments. A 25 mg aliquot of the biochars (AB, COF) or activated carbon (Cyclecarb® 301, as a control) were added to 10 ml medium in the Hungate tubes, prior to sterilization by autoclaving. After autoclaving and cooling down, 1 ml of mixed bacterial culture was added to the vials, and 10 mg/L of the pharmaceuticals or pesticides. Conditions tested were in the presence of 40 mM fumarate, in triplicate. Samples were incubated for 14 days prior to sampling for HPLC analyses and Bradford.

2.6 Pesticide and Pharmaceutical Extraction Procedure

For the extraction of the micropollutants, a modified QuEChERS method was used (Rejczak and Tuzimski, 2015; Lozowicka et al., 2016; Lehmann et al., 2018). In detail, 3 ml of supernatant was collected and centrifuged in an Eppendorf 5810 R centrifuge (Hamburg, Germany) for 15 min at 4,000 rpm. Next, an equal volume of acetonitrile (HiPerSolv, VWR, Leuven, Belgium) was added. After shaking briefly, salts were added [1.2 g anhydrous magnesium sulphate (Alfa Aesar, Haverhill, United States), 0.3 g sodium chloride (VWR), 0.3 g trisodium citrate dihydrate (Sigma-Aldrich) and 0.15 g disodium hydrogen citrate sesquihydrate (Sigma-Aldrich)]. The mixture was shaken vigorously for 5 min and centrifuged (5 min, 4,000 rpm). The supernatant was filtered with a 0.2 μm PTFE syringe filter (VWR) and transferred to a High-Performance Liquid Chromatography (HPLC) vial. Freshwater medium spiked with known concentrations of pharmaceuticals and pesticides, were used to obtain extraction recovery percentages. Blanks were run alongside as negative control.

2.7 High-Performance Liquid Chromatography Analyses

HPLC was performed using an ACE Equivalence C18 column (EQV-5C18-2,546, VWR, Leuven, Belgium; 4.6 × 250 mm, octadecyl as functional group, pore size of 11 nm, particle size of 5 μm, surface area of 280 m^2/g, a carbon load of 15%) and using the Hitachi Chromaster instrument consisting of the 5,160 pump, 5,280 autosampler, 5,310 column oven and 5,430 diode array detector (VWR, Oud-Heverlee, Belgium). The mobile phase used for ibuprofen and diclofenac consisted of 3:1 ACN:MetOH with a speed of 1 ml/min (Qin et al., 2012). For ibuprofen the retention time was 3.3 min, and peak measured at 264 nm. Diclofenac was measured at 276 nm after 3.13 min. For pirimicarb, a 30:70 Milli-Q water:ACN phase was used for 5 min (Peng et al., 2013). Thiacloprid was run in Milli-Q water:ACN with the following gradient:

0–3 min: 90:10; 3–10 min: 80:20; 10–15 min: 50:50; 15–17 min: 90:10 (Ying and Kookana, 2004). The retention time of pirimicarb was 4.2 min, for thiacloprid 14.7 min. Pirimicarb was monitored at 244 nm, thiacloprid at 242 nm. For each pollutant, concentrations of unknown samples were calculated using a 7-point calibration curve.

2.8 Bradford Protein Assay

Protein concentrations were determined by the Bradford method with bovine serum albumin (BSA, ThermoFisher Scientific, Massachusetts, United States) as a standard, using the Quick Start Bradford Dye Reagent (Bio-Rad, Hercules, CA, United States) for soluble protein quantification. First, a standard curve was made, diluting BSA in Milli-Q water (linear range from 125 to 2000 µg/ml). 50 µL of each solution was then mixed with 50 µL of a 1 M NaOH solution and vortexed. Afterwards, the dilutions were mixed with the Bradford dye, incubated for 5 min and the absorbance was measured at 595 nm using UV detector (Shimadzu UV-1602, Shimadzu, Kyoto, Japan). Medium was sampled from the vials or tubes and then vortexed for 30 s 500 µL NaOH was then added to 500 µL sample, then vortexed for 5 s 100 µL of this mixture was then added to 1 ml Bradford dye and after 5 min of incubation, the absorbance was measured at 595 nm.

2.9 Scanning Electron Microscopy

To evaluate cell attachment to the biochar or activated carbon, a sample of the biochar and activated carbon from the degradation experiments was prepared for scanning electron microscopy. Samples were fixed with 2.5% glutaraldehyde in 0.1 M phosphate buffer for 4 h at 4°C, then washed 3 times in 0.1 M phosphate buffer at 4°C for 10 min, dehydrated in an ethanol/water mixture of 50, 70, 80, 90, 95 and 100% for 10 min each (dehydration in 100% ethanol was done 3 times), and at last immersed twice for 30 s in pure hexamethyldisilazane (Sigma Aldrich, St Louis, MO, United States) followed by 10 min of air-drying. Before SEM analysis, the samples were sputter coated by an Auto Fine Coater (JFC-1300, JEOL, Peabody, United States) with a coater containing a gold target (81,001 Gold target (57 × 0.1), JEOL, Peabody, United States) and the analysis was done with a benchtop SEM (TM3000, Hitachi, Tokyo, Japan) at an acceleration voltage of 15 kV. At least 3 areas/sample were scanned. Images were processed and analyzed using the software ImageJ 2.0.0 (developed by National Institutes of Health, Bethesda, United States).

2.10 Fluorescence *In-Situ* Hybridization

Paraformaldehyde (PFA)-fixation was performed on biochar and Cyclecarb samples according to Amann et al., 1995. The samples were fixated and hybridized in Eppendorf tubes. A 1.4% paraformaldehyde (PFA) solution was added to the samples for 24 h at 4°C. Then, the tubes were shaken and the supernatant was removed. A washing step with 1 × PBS (pH = 7) was performed 3 times: 1 ml 1xPBS was added to each sample, then resuspended with a pipette tip and the supernatant was removed. 300 µL 1 × PBS was then added to the samples, with

the same amount of molecular biology grade 100% ethanol (not denatured), mixed well and stored at −20°C (Amann et al., 1995). The samples were then dehydrated by adding 50, 80 and 100% ethanol successively (3 min each) and air dried. Next, hybridization was performed on the samples. A 30% formamide (FA) solution was made by combining 270 µL of NaCl, 30 µL of Tris/HCl, 750 µL of ddH$_2$O, 450 µL of FA and 1.5 µL of 10% SDS. Afterwards, the solution was filter sterilized. 24 µL hybridization buffer was added to each dried sample, as well as 3 µL of each probe (six probes were added in total, concentration 50 ng/µL). The samples were then hybridized in a moisture chamber. The Eppendorf tubes were placed in a rack and silver foil, and consequently in a water bath at 46°C for 3 h. Afterwards, the formamide was washed off by pouring approximately 2 ml of washing buffer (0.02 M Tris-HCl; 0.01% SDS; 0.005 M EDTA; 0.1 M NaCl and ddH$_2$O) in the Eppendorf tubes. Samples were then placed in a water bath for 20 min at 48°C. Afterwards, the washing buffer was removed, the samples were washed with ddH$_2$O and air dried at room temperature. The samples were then placed in folded aluminum foil and stored at −20°C until microscopic examination. The probes that were used were the following (**Table 1**): Fluo-GEO3-A, Fluo-GEO3-B and Fluo-GEO3-A to target *Geobacter* species, with the helpers HGEO3-4 and HGEO3-4, and then also Cy3-EUB338 or Cy5-EUB338 to target most, synthesized by IDT (Coralville, United States). The samples were stained with DAPI (4′,6-diamidino-2-phenylindole) to stain all nucleic acids. Images were taken in a Leica TCS SP5 AOBS Spectral Confocal Microscope, equipped with four lasers (405, Ar, Kr/Ar, and He/Ne) (405, 561, and 633) and 4 prism spectrophotometer detectors. The objective used was a HCX APO L U-V-I 40.0 × 0.80. The software was the Leica Confocal Software (LCS) for multi-dimensional image series acquisition. The images were processed and analyzed using ImageJ 2.0.0.

2.11 Statistical Analysis

Statistical analysis was performed in SPSS (IBM Analytics, New York, United States). Independent sample t-tests and one-way or two-way ANOVA analysis were used for comparing group averages (using a significance level of $\alpha = 0.05$, $n = 3$ replicates). If the ANOVA result was significant, Tukey HSD was used as the post hoc test for all pairwise comparisons. Outliers were removed using a ±25 percent interquartile distance cut-off. All variables were checked for normality using the Shapiro-Wilk test and homogeneity of variances (Levene's test or Brown-forsythe).

3 RESULTS

3.1 Biochar Characterisation

The three types of biochar (AB, COF, and PDF) were characterized for their physical and chemical properties.

Results showed that the type of material has the greatest influence on the pH (**Figures 1A–C**) and conductivity (**Figures 1D–F**), more than the pyrolysis temperature. COF and PDF both had a basic pH (average 10.4 and 10,

TABLE 1 | Probes used for FISH.

Target	Probe	Sequence	Fluorochrome	Formamide (%)
Geobacter cluster A	GEO3-A	CCGCAACACCTAGTACTCATC	Fluorescein	30
Geobacter cluster B	GEO3-B	CCGCAACACCTAGTTCTCATC		
Geobacter cluster C	GEO3-C	CCGCAACACCTGGTTCTCATC		
Helper 1	HGEO3-3	GTTTACGGCGGGTACTACC		
Helper 2	HGEO3-4	CACTGCAGGGGTCAATAC		
Eubacteria	EUB338	TGAGGATGCCCTCCGTCG	ATTO550	30
Non-specific	None	ACTCCTACGGGAGGCAGC	Fluorescein	30
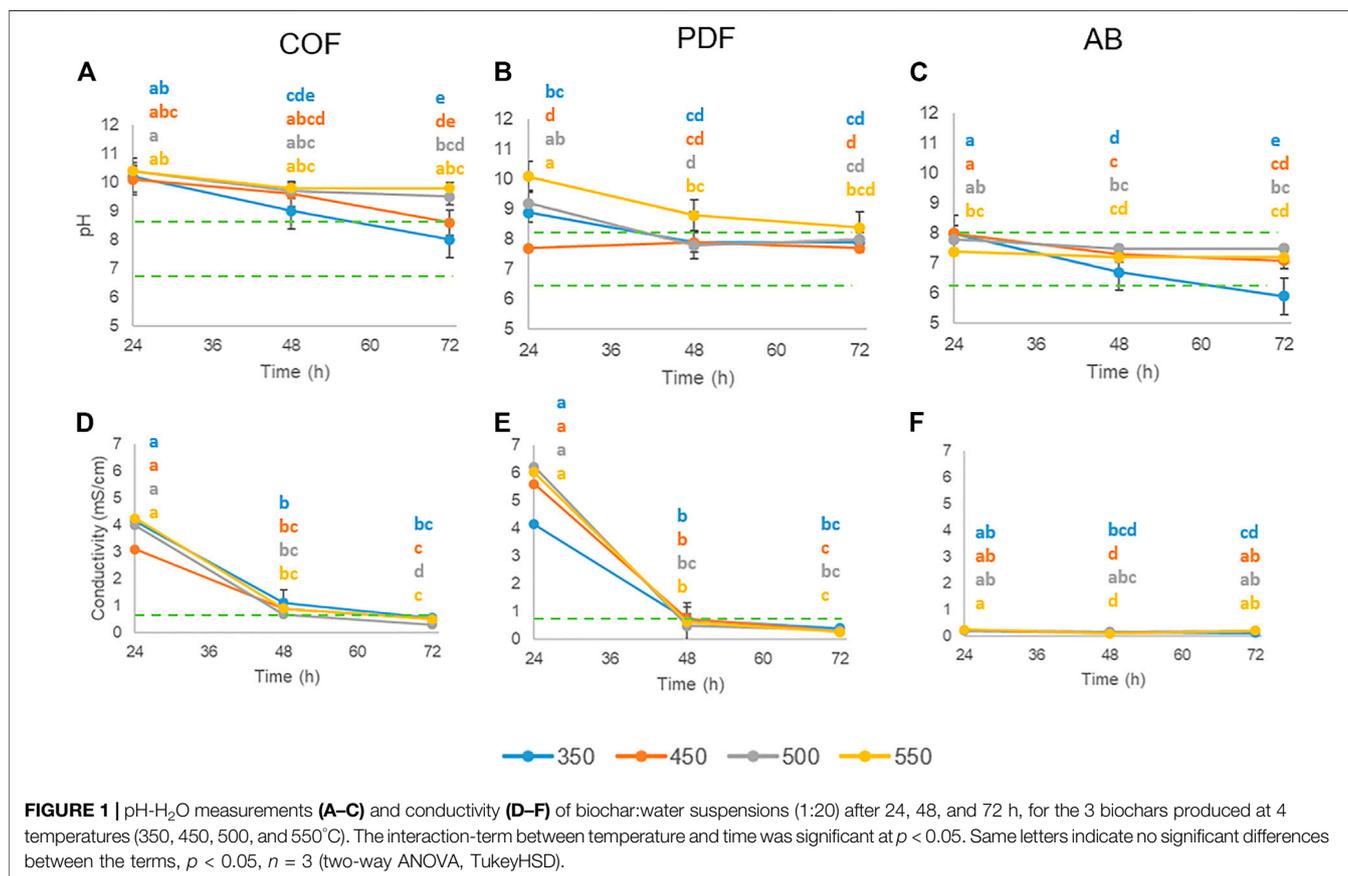
FIGURE 1 | pH-H$_2$O measurements **(A–C)** and conductivity **(D–F)** of biochar:water suspensions (1:20) after 24, 48, and 72 h, for the 3 biochars produced at 4 temperatures (350, 450, 500, and 550°C). The interaction-term between temperature and time was significant at $p < 0.05$. Same letters indicate no significant differences between the terms, $p < 0.05$, $n = 3$ (two-way ANOVA, TukeyHSD).

respectively at 550°C), and reached an average pH of 9.7 and 8.4 after 72 h. The pH of all three biochars decreased over time, and the higher the pyrolysis temperatures for PDF and COF the more alkaline pH. This was not the case for AB. For biochars produced at 450–550°C, all produced an average pH of 7.01–7.2 after 72 h.

Conductivity was initially high for PDF (6.04 mS/cm) and COF (4.3 mS/cm), having its maximum for 550°C (**Figures 1D–F**), but then decreased sharply after 48 h of shaking to average values of 0.26 mS/cm and 0.52 mS/cm for PDF and COF, respectively. This trend was not present for AB; the conductivity values were already low after 24 h, *i.e*,. an average of 0.24 mS/cm. Similar as for pH, conductivity is higher for higher pyrolyzation temperatures for COF and PDF. For AB, this trend was not observed.

Additionally, the leaching of anions, such as chloride, nitrate/nitrite, and sulphate was also measured. Large differences between materials and changes over time were observed (**Table 2**). PDF had very high initial chloride levels, up to 1760 mg/L after 24 h. When dried and resuspended for 72 h, a sharp decrease in chloride concentrations from >1,000 to 16–37 mg/L was seen. For COF an inverse relation was noticed between temperature and maximum leaching of chloride, with most Cl$^-$ (48.8 mg/L) at the lowest temperature.

The sulphate leaching was also high for PDF exceeding the sulphate norm in surface water (**Table 2**). There was no significant leaching of nitrate, only for PDF (550°C), with 13 mg/L nitrate. The higher the temperature, the more nitrate leaching was observed for COF (1 mg/L), but after 48 and 72 h, it

TABLE 2 | Leaching of chloride, nitrate and sulphate after 24, 48, and 72 h for the 3 types of biochars produced at 4 temperatures. The norms are the thresholds set in the VLAREM-II for surface water quality. Values above the norm are colored in red. Values with the same letter do not indicate a significant difference $p < 0.05$, $n = 4$. PDF: palm date fiber, COF: coffee bean husks, AB: waste wood mix.

Material	Temp (°C)	CHLORIDE (mg/L) norm: 120 mg/L			Nitrate (mg/L) norm: 10 mg/L			Sulphate (mg/L) norm: 90 mg/L		
		24 h	48 h	72 h	24 h	48 h	72 h	24 h	48 h	72 h
AB	350	7.37 b	3.89 a	3.89 b	0.41 a	0.34 a	0.78 ab	24.65 a	4.07 ab	5.35 a
—	450	10.1 b	3.32 a	3.32 a	0.56 a	0.54 a	6.32 a	29.59 a	3.24 ab	6.54 ab
—	500	8.62 b	3.31 a	3.31 b	0.4 a	0.55 a	0.58 b	25.45 a	2.98 b	2.13 b
—	550	17.74 a	4.55 a	4.55 b	0	0	0.36 b	21.26 a	4.32 a	2.43 b
COF	350	48.8 a	6.45 a	4.74 b	0.82 a	0.19 a	0	87.4 a	22.14 a	8.01 a
—	450	32.17 b	10.1 b	12.08 a	1.01 a	0.62 a	0.67 a	22.95 b	14.42 b	12.55 a
—	500	24.1 bc	10.33 b	11.76 a	1.12 a	0.64 a	0.54 a	29.18 b	15.3 b	12.92 a
—	550	26.8 c	9.66 b	12.03 a	1.42 a	0.44 a	0.53 a	76.39 a	15.7 b	12.74 a
PDF	350	999 b	82.26 b	22.83 c	0	1.11 b	0.29 a	547.7 c	66.64 a	29.95 a
—	450	1,609 a	176.07 a	36.75 a	0	0.7 c	0.9 bc	846.2 a	68.14 a	20.17 b
—	500	1760 a	183.5 a	37.56 b	0	0.38 a	0.81 bc	727.2 ab	109.7 b	33.92 a
—	550	1,548 a	69.4 b	16.87 b	13.53	0.67 c	0.83 bc	633.7 bc	123.28 b	33.57 a
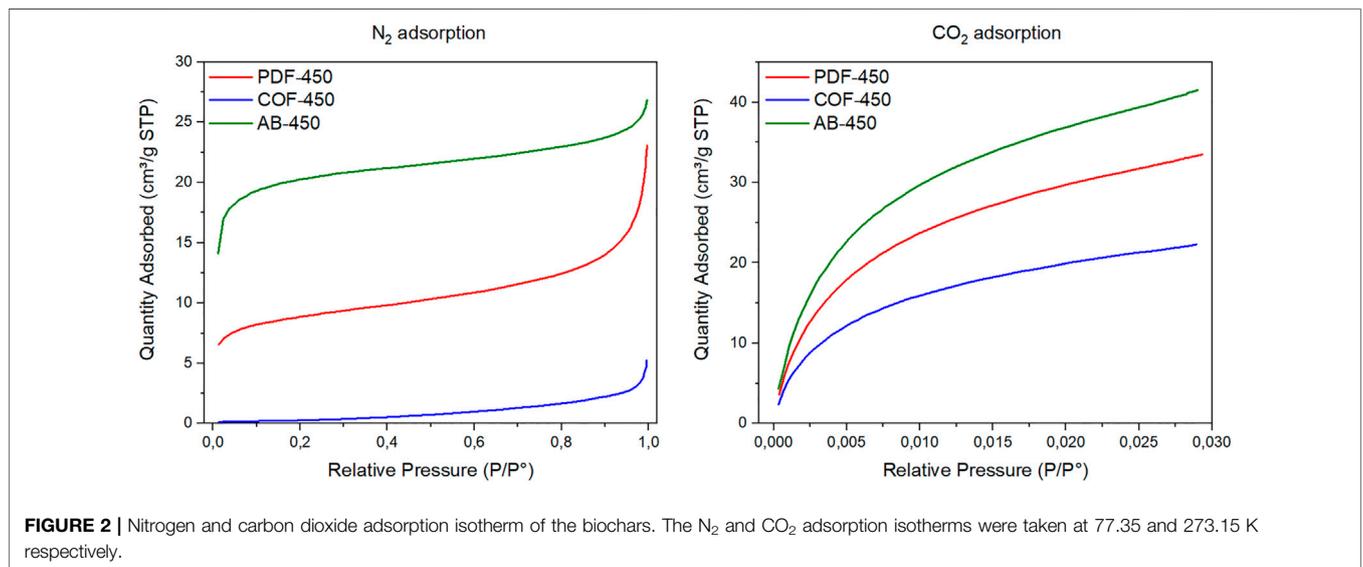
FIGURE 2 | Nitrogen and carbon dioxide adsorption isotherm of the biochars. The N_2 and CO_2 adsorption isotherms were taken at 77.35 and 273.15 K respectively.

decreased to half. Both AB and COF were the most suitable biochars, because leaching of Cl^-, nitrate and sulphate was well below the norms. AB-wood showed the least leaching from all 3 biochars.

The porosity and specific surface area, i.e., S_{BET}, of the biochars pyrolyzed at 450°C was evaluated by means of N_2 physisorption. The N_2 adsorption isotherms for the biochars are shown in **Figure 2**. The presence of micro porosity (pore width <2 nm) for the PDF-450 and AB-450 biochars was evidenced by sharp increase at low relative pressure, resembling a combination of a type I and II shape according to the IUPAC classification (Thommes et al., 2015). Instead, the COF-450 biochar "resembles" a type III isotherm, indicative of a non-porous sample and/or weak interaction of the COF-450s surface with the N2 adsorbate. The adsorption of the N_2 adsorbate at cryogenic temperature into (ultra)micropores is known to be kinetically disfavoured and can lead to an erroneous

interpretation of the sample's porosity (Jagiello et al., 2019). The biochars were also subjected to CO_2 adsorption at 273.15 K, **Figure 2**. Although the application of CO_2 as the adsorbate yields no information of meso- and/or macropores, it sheds light onto the (ultra)micropores in the sample. The CO_2 adsorption isotherms confirmed the presence of (ultra) micropores in both the PDF-450 and AB-450 biochar with the latter having a higher micropore volume. This observation was also confirmed by the higher quantity of adsorbed N_2 in the respective N_2 adsorption isotherms at low relative pressure. Interestingly, the COF-450 biochar also displayed a significant micropore volume in the CO_2 adsorption isotherm, invisible in its N_2 counterpart. This confirms that most of the micropore volume is simply inaccessible to the N_2 adsorbate, leading to a depressed adsorption plateau compared to the other two biochars. Hence, we can consider the N_2 adsorption isotherm of the COF-450 biochar to be of a combination of type II and type III as well. It is

TABLE 3 | Summary of the specific surface areas. The BET specific surface area (S_{BET}), the specific surface area ($S_{w < 2}$) correlated to micropores (pore width <2 nm) as calculated by the t-plot method, the specific surface area $S_{2<w < 300}$ of the meso- and macropores as calculated from the Barrett–Joyner–Halenda (BJH) method and the external surface area (S_{ext}) obtained from the N_2 adsorption isotherms. The specific surface area S_{BET, CO_2} has also been estimated from the CO_2 adsorption isotherms. All biochars were pyrolyzed at 450°C.

Adsorbate		N$_2$			CO$_2$
Sample	S_{BET} (m^2/g)	$S_{w < 2}$ (m^2/g)	$S_{2<w < 300}$ (m^2/g)	S_{ext} (m^2/g)	S_{BET, CO_2} (m^2/g)
PDF-450	32.9736	22.7141	6.244	4.0154	166.95
COF-450	2.1162	≈0	2.317	—	110.6
AB-450	78.2368	69.5666	4.461	4.2091	204.16

FIGURE 3 | Pore size distribution of the selected biochars. The pore size distribution is calculated from the N$_2$ adsorption isotherms by means of the BJH method.
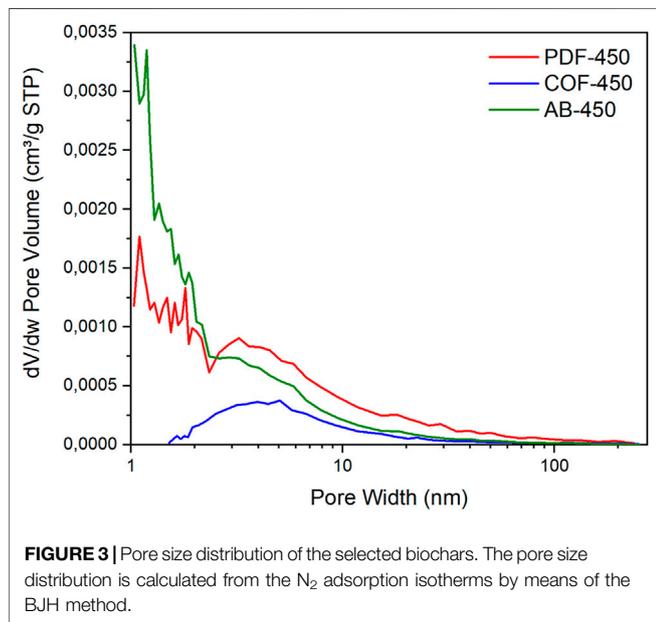
well known for biochars to be mainly (ultra)microporous and the creation of meso- and macropores occurs by activation rather than pyrolysis (Jagiello et al., 2019).

The N$_2$ adsorption isotherms were used to estimate specific surface area S_{BET} of the biochars by means of the Brunauer–Emmett–Teller theory, taking into consideration the Roucquerol approach for micropore-containing materials (Brunauer et al., 1938; Rouquerol et al., 2007). Subsequently, the t-plot method and BJH method were used to estimate the N$_2$-adsorbate-accessible micropore specific surface area $S_{w < 2}$ and meso- and macropore specific surface area $S_{2<w < 300}$ respectively (Barrett et al., 1951; Lippens and Boer, 1965). Ultimately, the exterior specific surface area was estimated. The results are summarized below in **Table 3**. The data reveals a high S_{BET} specific surface area of the AB-450 biochar similar to values reported in literature, e.g., an S_{BET} of 74 m^2/g for wood-based biochar pyrolyzed at approximately 400°C (Cederlund et al., 2016). The COF-450 has a low surface area, similar to the value of 2.63 m^2/g reported previously (Shafiq et al., 2019). The PDF-450 was found to be intermediate in terms of specific surface area. The palm date leaf-based biochars are reported to be highly dependent on the

pyrolysis temperature. Elnour et al., 2019 reported S_{BET} values of 5.535 m^2/g at 400°C pyrolysis and 123.63 m^2/g at 500°C (Elnour et al., 2019). These results place our PDF-450 biochar well within the set range. Interestingly, a higher meso- and macropore specific surface area was found for the PDF-450 biochar upon subtracting the contribution of the (N$_2$-adsorbate-accessible) micropores. This is visualized in the pore size distribution obtained from the BJH method, **Figure 3**. The AB-450 biochar's porosity is dominated by the micropores, as confirmed by the CO_2 adsorption isotherm. Meanwhile the exterior surface is rather similar to the PDF-450s. The COF-450 biochar has a lower surface area in either region compared to the other two. The specific surface area of the biochars was also estimated from the CO_2 adsorption isotherms as suggested in literature by extending the BET equation (Mukhtar et al., 2020). Higher S_{BET} and CO_2 values are found as the inaccessibility of the (ultra)micropores by the CO_2 adsorbate is no longer an issue in these conditions, revealing a large micropore specific surface area with an identical order. The trend in specific surface area, i.e., AB-450 > PDF-450 > COF-450, remains identical.

Other measured properties were yield and ash content (**Figure 4**). Yield decreased with an increasing pyrolysis temperature. However, only the yields at lower temperatures differed significantly from those at the highest temperatures. At lower temperatures, the yield of AB differed about 4% from the other two biochars. The relative ash levels increased with increasing temperature (**Figure 4**). The ash content of AB was on average 50% lower than COF and PDF due to the higher fraction of organic components. The moisture levels (average 2.47%) did not differ significantly between the different materials and temperatures.

3.2 Removal of Pesticides and Pharmaceuticals in Water in the Presence of Bacteria and Without Biochar

Without external electron shuttles like biochar, no significant degradation of thiacloprid and diclofenac was observed by either a mixed culture or *G. sulfurreducens* (**Figure 5**). For pirimicarb, a decrease in concentration was observed for *G. sulfurreducens* growing on acetate as electron donor, and for ibuprofen, both mixed and pure cultures growing on acetate and fumarate, or fumarate alone, could decrease ibuprofen concentrations.
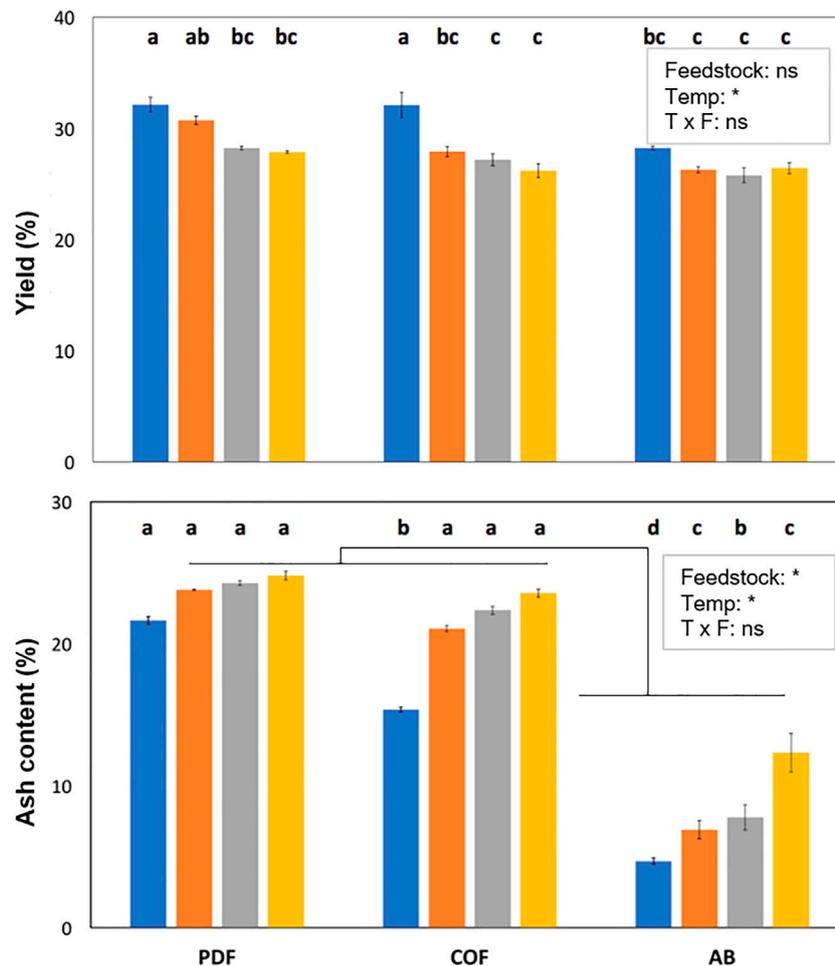
FIGURE 4 | Yield (%) and ash content (%) for the 3 biochars (PDF, COF, and AB) produced at 4 temperatures (350, 450, 500 and 550˚C). Bars with different letters indicate significant differences $p < 0.05$, $n = 3$ (two-way ANOVA, TukeyHSD). PDF: palm date fiber, COF: coffee bean husks, AB: waste wood mix.

Growth analysis based on protein concentration showed that the cells were not inhibited by 10 mg/L of the pollutants, and most growth was observed for the acetate and fumarate conditions (**Figure 6**), containing the donor/acceptor pair, followed by fumarate. For diclofenac, a mixed culture showed more growth than *G. sulfurreducens* for the acetate and fumarate condition (one-way ANOVA, $p < 0.05$), while for pirimicarb the pure strain formed more biomass correlating with the condition in which most degradation was measured. No significant difference between pure or mixed culture was observed for thiacloprid and ibuprofen.

3.3 Removal of Pesticides and Pharmaceuticals in Water With Bacteria and With Biochar

When comparing the total pesticide and pharmaceutical concentrations in the medium after 14 days in the presence of biochar or GAC (**Figure 7**), concentrations were significantly lower for all test conditions compared to the no-char control. For pirimicarb this was due to sorption mainly, as the control condition (dead cells) also showed significant pirimicarb removal without metabolically active cells. For the other conditions, there was a distinction between removal efficiency in the presence of active mixed culture, or dead cells. Cyclecarb was the most efficient in pesticide and pharmaceutical removal for all tested conditions with no distinction between alive or dead cells. Among the biochars, AB showed higher removal efficiencies than COF, especially for diclofenac (5 mg/L vs. < 1 mg/L). For thiacloprid in the mixed culture condition, 2.3 mg/L was remaining for AB, compared to 4.2 mg/L for COF, and for ibuprofen this was 2.7 mg/L vs. 3.9 mg/L for AB and COF, respectively. HPLC-chromatograms also showed degradation intermediates for thiacloprid, in particular for thiacloprid-amide based on overlapping retention time and UV-absorbance spectrum comparison to the authenticated standard (**Supplementary Figure S2**).

FIGURE 5 | Concentrations of pesticides and pharmaceuticals in freshwater medium after 14 days. Values represent means of triplicates ±SD. Gs = *G. sulfurreducens*; MC = Mixed culture. *indicates a significant difference at $p \leq 0.05$, $n = 3$ (one-way ANOVA, factor Bacteria).
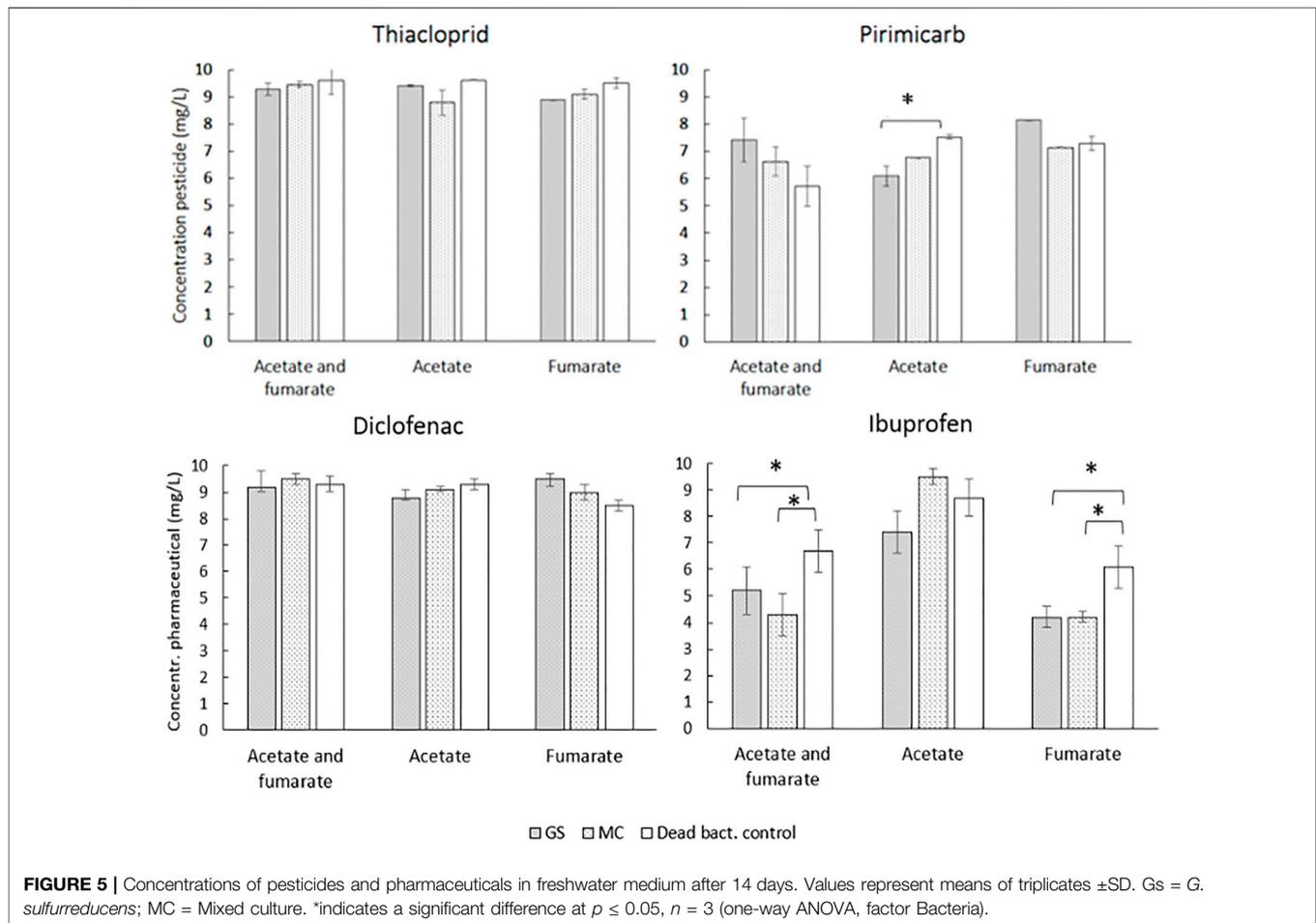
3.4 Fluorescence *In Situ* Hybridization Shows Colonization of Mixed Culture on Biochar Particles and GAC

The biofilms developed on the biochar and GAC particles exposed to 10 mg/L pirimicarb were characterized by FISH. The biochar particles with mixed culture showed the presence of *G. sulfurreducens*, as well as Eubacteria (**Figure 8A** and **Supplementary Figure S1A**), more than on the activated carbon (**Figure 8C**). When comparing to the control biochar particle or GAC (dead cells), almost no Eubacteria and no *G. sulfurreducens* were found (**Figures 8B,D** and **Supplementray Figure S1B**).

3.5 Scanning Electron Microscopy

Scanning electron microscopy (SEM) images were taken from biochar particles at the end of the degradation assays, to gain additional information on the attachment of the bacteria. The biochar with mixed culture showed a dense coverage with bacteria or imprints thereof (**Figures 9A,B**, representative of multiple scanned areas/biochar particle), while the no-bacteria control (**Figures 9C,D**) shows as expected a complete absence of bacteria. The cell bodies have average lengths of 1.7 μm and widths of 0.4 μm, which are the typical cell sizes for *G.*

sulfurreducens. Together, the images of SEM and FISH suggest that the biochars can serve as a suitable surface for bacterial attachment.

4 DISCUSSION

4.1 Biochar Characterization

The objectives of this study were twofold, 1) characterization of biochars made from waste-material and pyrolysed at different temperatures and 2) testing their suitability for use in the remediation of micropollutants in (waste) water. We showed that COF and AB were the two most suitable biochars of the three based on neutral pH, conductivity and anion leaching values below the norm. Pyrolysis temperature had on some properties an effect and this was also feedstock dependent. In the presence of biochar (AB or COF) and a mixed bacterial culture, the removal of thiacloprid, pirimicarb, diclofenac and ibuprofen was significantly higher compared to the non-biochar controls. When compared to CycleCarb activated carbon, or dead cell controls, not only sorption of the pollutants took place, but a combination of adsorption and degradation was seen. This was additionally confirmed by looking at the HPLC chromatogram of thiacloprid; identification of additional peaks indicative of

FIGURE 6 | Bacterial growth measured after a 2-week incubation period. **indicates statistical difference ($p \leq 0.01$, $n = 3$, one-way ANOVA, factor medium). Gs = *G. sulfurreducens*; MC = Mixed culture.
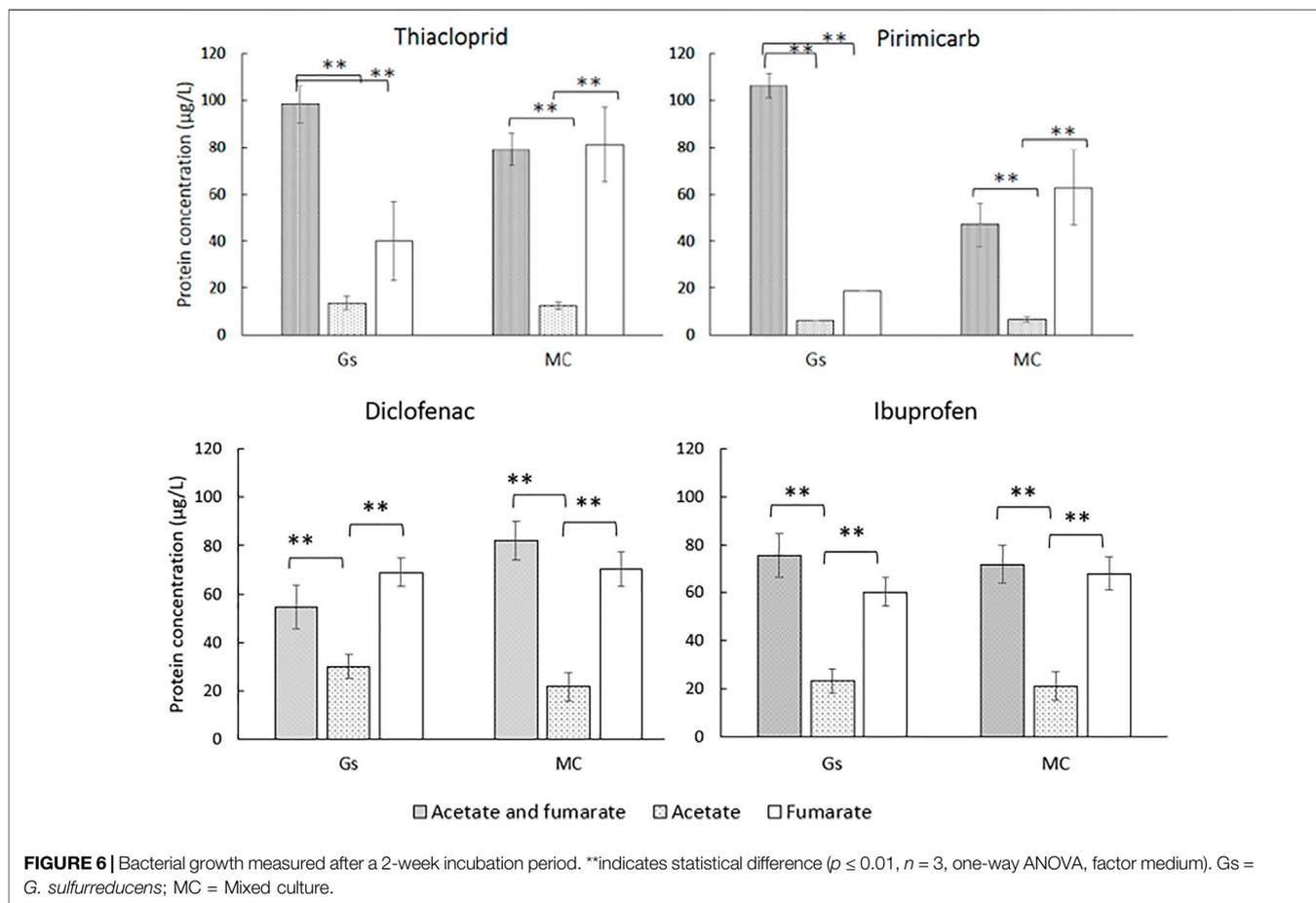
degradation intermediates. In the following sections, we discuss the differences between the biochars in terms of the measured physical and chemical properties, and their make-up including functional groups. We assessed the potential of these specific types of low-cost waste-material biochar (AB-wood, coffee bean husks, date palm) as a sustainable and much cheaper alternative to activated carbon, pre-treated activated coffee bean biochar (Maged et al., 2021) or wood biochar (Cederlund et al., 2016) and tested this in combination with pirimicarb, thiacloprid, diclofenac and ibuprofen degradation. Even though the pesticides are commonly found in wastewater, almost nothing is known about their biodegradation, in contrast to the pharmaceuticals diclofenac and ibuprofen which have already been investigated in more detail.

For both COF and PDF, carbonates leaching from the ash explained the initial alkaline pH, but after the wash at 24 h, not much more alkaline compounds leached from the char. The pH did not stabilize for PDF, COF and AB350 samples after 72 h, so the effect of leaching should be measured for 96 h or longer. In Flanders (Belgium), VLAREM sets the basic environmental quality standard for pH of surface water at 6.5–8.5. AB meets this standard for all temperatures except AB350 after 72 h (5.9). PDF also meets this basic standard except for PDF-550 after 24 h (10.0) and for PDF-500 after 24 h (9.2). COF has too alkaline pH for 500 and 550°C produced biochar.

There was a negative correlation between conductivity and time for COF and PDF. On the other hand, for the same materials, there was an increase in conductivity with an increasing pyrolysis temperature. The downward trend is the result of leaching of salts such as NaCl and KNO₃. The increase in conductivity at increasing temperature is correlated with a relative increase in ash content at higher temperatures when the fraction of salts increases (Ronsse et al., 2013). These trends are not present for AB samples which is explained by its low ash content. The high degree of aromaticity of the AB biochars therefore indicates a high electrical (dry) conductivity of the material, and this is very conducive for biodegradation (Yu et al., 2015). The basic environmental quality standard for the conductivity of surface water, as determined according to VLAREM, is 0.6 mS/cm. After 72 h this criterium was met for all three biochars.

The highest porosity was found for the AB biochar, followed by PDF and COF biochar, respectively, with the microporosity dominating for all. The selected pesticide and drug molecules are able to adsorb into the wider micropores due to the small molecular sizes, i.e., 1.03–1.39 nm length and 0.79–0.95 nm width (Chen et al., 2004; Vergili, 2013; Jia et al., 2018). The three biochars have comparable specific surface area's compared to expanded perlite zeolite (S_{BET} 2.3 m²/g) and silica (S_{BET} 7.4 m²/g) (Rafatullah et al., 2010).

FIGURE 7 | Pesticide and pharmaceutical concentrations measured in the medium after 2 weeks. MC = Mixed culture. Shown values are means of triplicates ±SD. **Indicates a statistical difference with $p \leq 0.01$ (one-way ANOVA, factor Bacteria). Line plot and right axis in blue shows the protein concentrations, letters indicate significant differences compared to the no biochar control ($p < 0.05$, $n = 3$).

Yields were negatively correlated with temperature. With an increasing temperature, more degradation of lignocellulose occurs which reduces the yield (Gai et al., 2014). Derived from the ash content, AB contains far fewer inorganic components compared to the other two biochars that also explain the lower yield and different influence on pH changes. The relative ash content increases with increasing pyrolysis temperature, which is to be expected, as the ash remains in the solid fraction while the organic components experience thermal decomposition (Ronsse et al., 2013). However, this trend was not significant for COF and PDF due to the small sample size. The ash content of AB was lower compared to the other two materials due to the higher fraction of organic components.

Striking was the high Cl-leaching of PDF, which can be explained by the fact that date palm (PDF) contains a high concentration of KCl in its biomass (Agoudjil et al., 2011), hence chloride-rich material has to be avoided as feedstock. For COF, the decreasing trend in leaching, may be explained by an increase in volatilisation of chloride components at higher temperatures. The chloride leaching in PDF exceeds the basic environmental quality standard of 120 mg/L (as determined according to VLAREM), and was therefore not used in the following degradation tests. PDF had also a higher nitrate leaching than the other two biochars. The increasing trend

observed for COF indicates an increased exposure of nitrates with an increasing pore surface. The three biochars were however all below 10 mg/L leaching and thus meet the basic environmental quality standards of VLAREM.

In summary, the results showed that only AB and COF met VLAREM's environmental quality standards for both pH, leaching and conductivity in solution. A too high pH, chloride leaching and sulfate leaching was observed for PDF. Therefore, this type of biochar was no longer considered for the degradation experiments. The final temperature, 450°C was chosen for the pesticide, pharmaceutical removal experiments because there was no additional gain in yield compared to 500 and 550°C produced biochars, and the 350°C biochar had initially higher Cl⁻ and sulphate concentrations than the 450°C biochar.

4.2 Removal of Pesticides and Pharmaceuticals in Water With Bacteria

The degradation of diclofenac and thiacloprid by electroactive bacteria in the absence of any conductive material or substrate, was minimal. Although the bacteria grew abundantly (best on medium with both an extra electron acceptor and donor), little breakdown was observed regardless of the medium. When
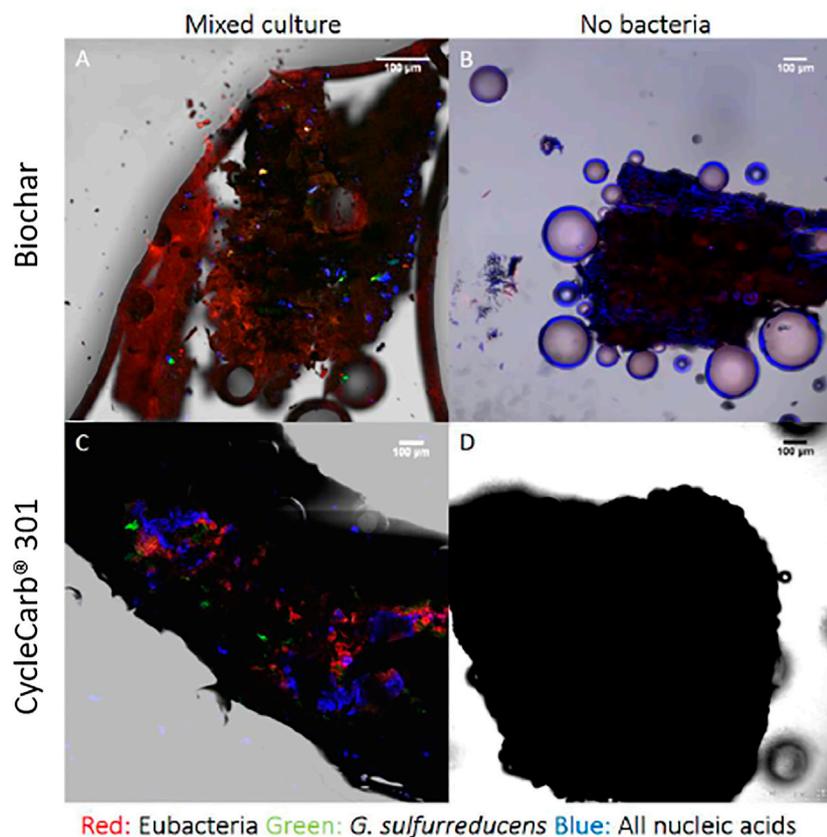
FIGURE 8 | Fluorescence in situ hybridization images. All particles were exposed to 10 mg/L pirimicarb with alive mixed cultures or dead-bacteria controls. **(A)** biochar with mixed culture; **(B)** dead bacteria; **(C)** Cyclecarb® 301 with mixed culture; **(D)** Control Cyclecarb® 301 with dead bacteria. DAPI (blue signal) shows all nucleic acids; *G. sulfurreducens* (green signal); Eubacteria (red signal).

comparing to other studies that used aerobic digestion for the breakdown of diclofenac, the results are variable. One study by Ternes et al., 2002, stated that the biodegradation of diclofenac is low (Ternes et al., 2002). In another 161-day study by Lahti and Oikari, 2011, it was shown that in the long-term diclofenac is broken down with 26% in nonsterile conditions (Lahti and Oikari, 2011). Carballa et al., 2004 showed that diclofenac can be removed from wastewater by anaerobic digestion, though it also mentions that the used sludge needed some adaptation before diclofenac was effectively broken down (Carballa et al., 2004). The study from Lahti and Oikari, 2011 confirmed that the biotransformation of diclofenac is highly dependent on environmental factors, experimental design and the source of inoculum. A recent study by Żur et al. (2021) found four new bacterial strains capable of diclofenac degradation (Żur et al., 2021). They also stated that diclofenac degradation is strain-specific. We used a natural inoculum of bacteria from the Stiemerbeek, a stream receiving sewage overflow regularly but the indigenous bacteria do not show high natural degradation capacity for the tested micropollutants in a 14-day degradation window. Interestingly, both the pure culture and mixed culture showed degradation potential for ibuprofen and pirimicarb. This is better than the results obtained by Musson et al., 2010,

who tested the biodegradation of ibuprofen by activated sludge and over 112 days, no significant degradation was noted under these conditions (Musson et al., 2010). Ibuprofen is a highly branched structure with substitutions in the para-position of the aromatic ring which may cause its resistance to biodegradation. Though, recent work has shown that biodegradation is possible by a specific bacterial strain, *Sphingopyxis granuli* RW412, isolated from sediments of the River Elbe (Aguilar-Romero et al., 2021). The strain first uses a CoA ligation, followed by aromatic ring activation by a dioxygenase and retroaldol cleavage to produce 4-isobutylcatechol and propionyl-CoA (Aguilar-Romero et al., 2021). Also, in ibuprofen-spiked effluent from a municipal wastewater treatment plant, this strain remained active and ibuprofen removal was 7 times faster than indigenous microbes. So in future it can be interesting to combine this well-adapted strain with electroactive material, biochar, in wastewater treatment systems.

So far, there is very limited information available about the degradation of pirimicarb (Chen et al., 2009; Soloneski and Larramendy, 2015) and thiacloprid by microorganisms in soil or water (Pang et al., 2020). The only pirimicarb metabolites found in literature so far for come from mammal studies,
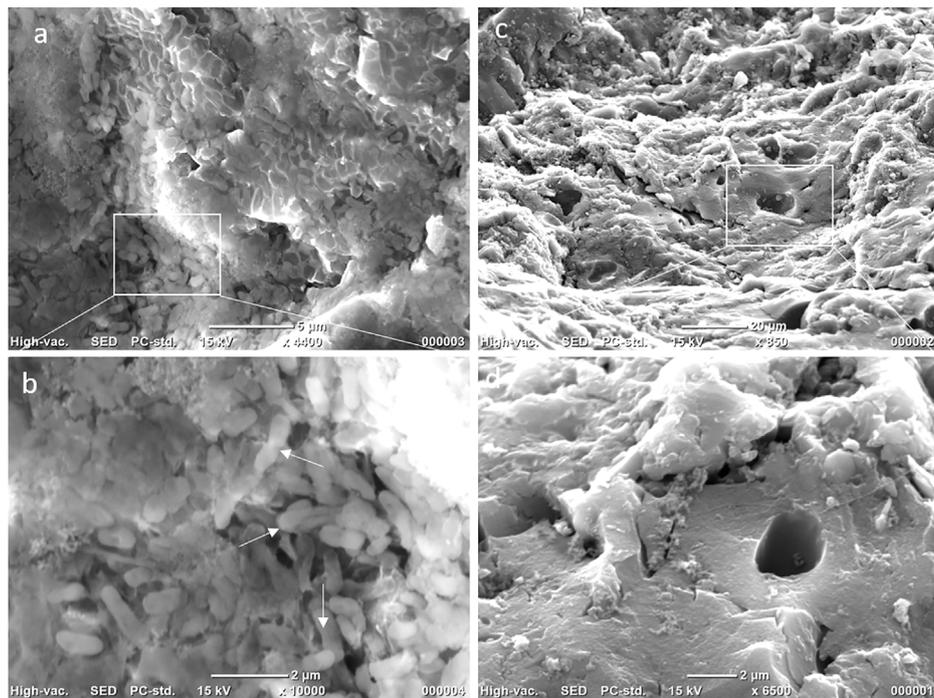
FIGURE 9 | (A) Scanning electron microscopy image of biochar particles with a mixed culture, and **(B)** enlarged image of the white rectangle area. **(C)** No-bacteria reference biochar particle and **(D)** zoomed in on the area in the white box. White arrows point to representative bacterial cells.

where was stated that phenolic components of pirimicarb are found with modifications of the alkyl constituents of the aromatic moiety (Baron, 1978). For thiacloprid, a degradation route has been described to occur via hydroxylation of thiacloprid into 4-hydroxyl mercaptoimiacloprid, or by hydrolysis of thiacloprid to thiacloprid amide, and lastly an attack by a nitrile hydratase (Pang et al., 2020). The first route was catalysed by a *Maltophilia oligotrophomonas* with a degradation rate of >90% in 30 h starting from 0.63 mmol/L thiacloprid, and the second reaction has been described to be used by *Variovorax boronicumulans* and *Ensifer meliloti*. *Microvirga flocculans* has been described to use a nitrile hydratase to degrade thiacloprid (Pang et al., 2020). So far no strain has been found to completely mineralize thiacloprid beyond its amide metabolite (Pang et al., 2020). In our study, we confirmed that the pure strain *G. sulfurreducens* and the mixed culture formed thiacloprid-amide as an intermediate. No other peaks which could point to degradation products of pirimicarb were detected. In one study by Chen et al., 2009, they found that the main pirimicarb degradation product by soil microorganisms was 2-dimethylamino-5,6-dimethyl-4-hydroxypyrimidine (Chen et al., 2009). In another study by Lan et al., 2006, they genetically engineered *E. coli* BL-21 in hope to detoxify pirimicarb by adding the carboxylesterase B1 gene from *Culex pipiens* (Lan et al., 2006). They purified the resulting enzyme and tested it in an insect bioassay where they exposed mosquito larvae to a pirimicarb solution which

included the B1 enzyme. However, little pirimicarb degradation was seen.

4.3 Removal of Pesticides and Pharmaceuticals in Water With Bacteria and Biochar

In comparison to the bacteria alone, we noticed that with addition of conductive material, AB-wood biochar, COF biochar or Cyclecarb® 301, a minimum 50% removal of all micropollutants was achieved. The main effect that is observed in these experiments is the sorption by the biochars or activated carbons. Similar (but less than) to the activated carbons, the biochar has a reasonable large specific surface area, is mainly microporous, and has enriched surface functional groups that make it possible to use it as an adsorbent. The main mechanisms for adsorption onto biochar are electrostatic interaction, hydrophobic effects, hydrogen bonds and pore-filling (Tan et al., 2015). The difference between adsorption by COF or AB in absence of the microbes is only significant for the diclofenac. A plausible explanation could be its relatively low dipole moment, compared to the other drug and pesticides, leading to a more preferential surface-adsorbate interaction on the more aromatic AB biochars. As high amounts of pollutants are adsorbed, the adsorption may also lead to a competition between the pollutant and the bacteria. At the same time there is also the competition between the pollutant and other organic compounds available in the solution (Ternes et al., 2002).

The concentrations of thiacloprid, diclofenac and ibuprofen, measured in the AB and COF samples, were lower in the presence of a mixed culture than in the dead-cell control samples. This indicates that not only adsorption but also a potential breakdown of these micropollutants takes place. For diclofenac specifically, biodegradation might be a more promising way to lower diclofenac concentrations in water, as adsorption onto solids such as GAC of biochar is low at neutral pH and minimal at low pH (where they will occur as ions) (Aissaoui et al., 2017). In a study by Lonappan et al. a biochar made of pine wood—somewhat similar to our AB wood biochar—was used for the adsorption of diclofenac. Batch adsorption tests were performed with pine wood biochar (2 g/L) in Milli-Q water and 500 µg/L or 10 mg/L diclofenac. The maximum removal efficiency was obtained after 4.5 h, with 40% removal compared to the initial concentration. Diclofenac has a negative charge, and could bind to the positive charge on the biochar surface, *e.g.,* hydroxyl groups that create positive surface radicals (Lonappan et al., 2018). In 2000, Radovic et al. investigated the effect of bacteria in the presence of activated carbon. Their results showed that colonization of carbon by bacteria decreased the porosity, but that the adsorption capacity was increased (Radovic et al., 2000). Bautista-Toledo et al., agreed to some extend by showing that bacteria on activated carbon can accelerate adsorption of different compounds, mainly due to the higher surface hydrophobicity (Bautista-Toledo et al., 2008). Also, Yu et al., 2015, showed that enhanced bacterial growth and reductive dechlorination of pentachlorophenol by *G. sulfurreducens* was measured in the presence of biochar (Yu et al., 2015). A conformation of the colonization potential of the biochars in our study was provided by SEM and FISH. The colonization was clearly visible on the biochar particles in comparison to the control, and cell sizes combined with the confirmation by *Geobacter* specific probes indicated the presence of the *Geobacter* type of electroactive bacteria.

A longer contact time between the bacteria and the adsorbed pollutants, and the presence of reactive side-groups provided by the biochar particles, are the likely explaining mechanisms that could have enhanced degradation. For thiacloprid we were able to detect peaks in the HPLC chromatogram with the same retention time and UV-spectrum for thiacloprid-amide. It needs to be confirmed in future follow-up studies by looking more in detail to the degradation products, metabolic pathways, and fraction of pollutant/metabolite adsorbed on the biochar particle whether this hypothesis is true. Additionally, focusing on the functional side-groups of the biochars, and modification of the biochar can additionally speed-up degradation (Cederlund et al., 2016; Maged et al., 2021). Also, the starting material, *e.g.,* many aromatic rings in AB-wood biochar, can have a positive impact on biodegradation, sorption and colonization compared to other biochars (COF) (Dai et al., 2017).

In general, there is still substantial research that needs to be performed, but we have provided first promising results for waste-wood biochar material. The AB-wood and coffee bean biochar showed the most promising results for micropollutant removal, and can be used as a sustainable alternative to non-conductive filling material (sand, gravel) in wastewater treatment

plants. We performed the experiments with indigenous bacterial strains, but for the best results, bacteria need to have been pre-adapted to the pharmaceuticals or pesticides for a longer time. At the time of performing these experiments, the ibuprofen-degrading strain (Aguilar-Romero et al., 2021) was not yet discovered, and also the microbial degradation and biochemical mechanisms of neonicotinoid degradation were elusive (Pang et al., 2020). Furthermore, isolations of bacteria from thiacloprid, pirimicarb or pharmaceutical polluted water can also lead to the discovery of new degradative strains, which can be used in future biochar-enhanced remediation experiments, especially in the case of pirimicarb with little knowledge on its degradation. Experiments can also be set up in simple microbial fuel cells (MFCs) with biochar before moving to constructed wetlands. For example, Wang et al., 2015, tested the removal of 26 micropollutants in single- or two chamber MFCs, using carbon cloth as the anode. Their results show that the removal of positively charged micropollutants was higher, and that the properties of the compounds determined how well they were removed (Wang et al., 2015). So more mechanistic insights can be obtained from these BES systems and also answers as to how the pesticides and pharmaceuticals are metabolized by the bacteria. The BES can also be equipped with plants, as root exudates can provide nutrients for the bacteria but also allelochemicals which can enhance degradation. For example, for the degradation of azo dyes in a MFC, it was found that a co-substrate was required for the dye degradation. Here, the co-substrate acted as electron donor for the electroactive bacteria on the anode, and the electroactive bacteria were then able to use part of these electrons to reduce azo dyes (Liu et al., 2009; Stevens-Garmon et al., 2011). With prototypes of BES systems in our lab, combined with cyclic voltammetry measurements, we will be able to gain new insights in biochar-enhanced removal of micropollutants from wastewater in the short future.

DATA AVAILABILITY STATEMENT

The original contributions presented in the study are included in the article/**Supplementary Material**, further inquiries can be directed to the corresponding authors.

AUTHOR CONTRIBUTIONS

FUNDING

UHasselt, and ST was supported by the Methusalem grant 08M03VGRJ provided by JV.

ACKNOWLEDGMENTS

SUPPLEMENTARY MATERIAL

The Supplementary Material for this article can be found online at: https://www.frontiersin.org/articles/10.3389/fenvs.2022.814267/full#supplementary-material

REFERENCES

Agoudjil, B., Benchabane, A., Boudenne, A., Ibos, L., and Fois, M. (2011). Renewable Materials to Reduce Building Heat Loss: Characterization of Date palm wood. *Energy Build.* 43, 491–497. doi:10.1016/j.enbuild.2010.10.014

Aguilar-Romero, I., De la Torre-Zúñiga, J., Quesada, J. M., Haïdour, A., O'Connell, G., McAmmond, B. M., et al. (2021). Effluent Decontamination by the Ibuprofen-Mineralizing Strain, Sphingopyxis Granuli RW412: Metabolic Processes. *Environ. Pollut.* 274, 116536. doi:10.1016/j.envpol.2021.116536

Aguirre-Sierra, A., Bacchetti-De Gregoris, T., Berná, A., Salas, J. J., Aragón, C., and Esteve-Núñez, A. (2016). Microbial Electrochemical Systems Outperform Fixed-Bed Biofilters in Cleaning up Urban Wastewater. *Environ. Sci. Water Res. Technol.* 2, 984–993. doi:10.1039/c6ew00172f

Aissaoui, S., Ouled-Haddar, H., Sifour, M., Harrouche, K., and Sghaier, H. (2017). Metabolic and Co-Metabolic Transformation of Diclofenac by Enterobacter Hormaechei D15 Isolated from Activated Sludge. *Curr. Microbiol.* 74, 381–388. doi:10.1007/s00284-016-1190-x

Amann, R. I., Ludwig, W., and Schleifer, K. H. (1995). Phylogenetic Identification and *In Situ* Detection of Individual Microbial Cells without Cultivation. *Microbiol. Rev.* 59, 143–169. doi:10.1128/mmbr.59.1.143-169.199510.1128/mr.59.1.143-169.1995

Baron, R. L. (1978). Terminal Residues of Carbamate Insecticides. *Pure Appl. Chem.* 50, 503–510. doi:10.1351/pac197850050503

Barrett, E. P., Joyner, L. G., and Halenda, P. P. (1951). The Determination of Pore Volume and Area Distributions in Porous Substances. I. Computations from Nitrogen Isotherms. *J. Am. Chem. Soc.* 73, 373–380. doi:10.1021/ja01145a126

Bautista-Toledo, M. I., Méndez-Díaz, J. D., Sánchez-Polo, M., Rivera-Utrilla, J., and Ferro-García, M. A. (2008). Adsorption of Sodium Dodecylbenzenesulfonate on Activated Carbons: Effects of Solution Chemistry and Presence of Bacteria. *J. Colloid Interf. Sci.* 317, 11–17. doi:10.1016/j.jcis.2007.09.039

Borjas, Z., Esteve-Núñez, A., and Ortiz, J. M. (2017). Strategies for Merging Microbial Fuel Cell Technologies in Water Desalination Processes: Start-Up Protocol and Desalination Efficiency Assessment. *J. Power Sourc.* 356, 519–528. doi:10.1016/j.jpowsour.2017.02.052

Brunauer, S., Emmett, P. H., and Teller, E. (1938). Adsorption of Gases in Multimolecular Layers. *J. Am. Chem. Soc.* 60, 309–319. doi:10.1021/ja01269a023

Carballa, M., Omil, F., Lema, J. M., Llompart, M., Garcı́a-Jares, C., Rodrı́guez, I., et al. (2004). Behavior of Pharmaceuticals, Cosmetics and Hormones in a Sewage Treatment Plant. *Water Res.* 38, 2918–2926. doi:10.1016/j.watres.2004.03.029

Cederlund, H., Börjesson, E., Lundberg, D., and Stenström, J. (2016). Adsorption of Pesticides with Different Chemical Properties to a Wood Biochar Treated with Heat and Iron. *Water Air Soil Pollut.* 227, 203. doi:10.1007/s11270-016-2894-z

Chen, S., Rotaru, A.-E., Shrestha, P. M., Malvankar, N. S., Liu, F., Fan, W., et al. (2014). Promoting Interspecies Electron Transfer with Biochar. *Sci. Rep.* 4, 5019. doi:10.1038/srep05019

Chen, S., Taylor, J., Mulford, L., and Norris, C. (2004). Influences of Molecular Weight, Molecular Size, Flux, and Recovery for Aromatic Pesticide Removal by Nanofiltration Membranes. *Desalination* 160, 103–111. doi:10.1016/s0011-9164(04)90000-8

Chen, T., Fu, F., Chen, Z., Li, D., Zhang, L., and Chen, G. (2009). Study on the Photodegradation and Microbiological Degradation of Pirimicarb Insecticide by Using Liquid Chromatography Coupled with Ion-Trap Mass Spectrometry. *J. Chromatogr. A* 1216, 3217–3222. doi:10.1016/j.chroma.2009.02.022

Dai, Z., Barberán, A., Li, Y., Brookes, P. C., and Xu, J. (2017). Bacterial Community Composition Associated with Pyrogenic Organic Matter (Biochar) Varies with Pyrolysis Temperature and Colonization Environment. *Msphere* 2, e00085–17. doi:10.1128/msphere.00085-17

de Souza, R. M., Seibert, D., Quesada, H. B., de Jesus Bassetti, F., Fagundes-Klen, M. R., and Bergamasco, R. (2020). Occurrence, Impacts and General Aspects of Pesticides in Surface Water: A Review. *Process Saf. Environ. Prot.* 135, 22–37. doi:10.1016/j.psep.2019.12.035

Elnour, A. Y., Alghyamah, A. A., Shaikh, H. M., Poulose, A. M., Al-Zahrani, S. M., Anis, A., et al. (2019). Effect of Pyrolysis Temperature on Biochar Microstructural Evolution, Physicochemical Characteristics, and its Influence on Biochar/Polypropylene Composites. *Appl. Sci.* 9, 1149. doi:10.3390/app9061149

Gai, X., Wang, H., Liu, J., Zhai, L., Liu, S., Ren, T., et al. (2014). Effects of Feedstock and Pyrolysis Temperature on Biochar Adsorption of Ammonium and Nitrate. *Plos One* 9, e113888. doi:10.1371/journal.pone.0113888

Jagiello, J., Kenvin, J., Celzard, A., and Fierro, V. (2019). Enhanced Resolution of Ultra Micropore Size Determination of Biochars and Activated Carbons by Dual Gas Analysis Using N2 and CO2 with 2D-NLDFT Adsorption Models. *Carbon* 144, 206–215. doi:10.1016/j.carbon.2018.12.028

Jain, A., and He, Z. (2018). Cathode-enhanced Wastewater Treatment in Bioelectrochemical Systems. *Npj Clean. Water* 1, 23. doi:10.1038/s41545-018-0022-x

Jia, P., Tan, H., Liu, K., and Gao, W. (2018). Removal of Methylene Blue from Aqueous Solution by Bone Char. *Appl. Sci.* 8, 1903. doi:10.3390/app8101903

Kozyatnyk, I., Oesterle, P., Wurzer, C., Mašek, O., and Jansson, S. (2021). Removal of Contaminants of Emerging Concern from Multicomponent Systems Using Carbon Dioxide Activated Biochar from Lignocellulosic Feedstocks. *Bioresour. Technol.* 340, 125561. doi:10.1016/j.biortech.2021.125561

Lahti, M., and Oikari, A. (2011). Microbial Transformation of Pharmaceuticals Naproxen, Bisoprolol, and Diclofenac in Aerobic and Anaerobic Environments. *Arch. Environ. Contam. Toxicol.* 61, 202–210. doi:10.1007/s00244-010-9622-2

Lan, W. S., Gu, J. D., Zhang, J. L., Shen, B. C., Jiang, H., Mulchandani, A., et al. (2006). Coexpression of Two Detoxifying Pesticide-Degrading Enzymes in a Genetically Engineered Bacterium. *Int. Biodeterior. Biodegr.* 58, 70–76. doi:10.1016/j.ibiod.2006.07.008

Lehmann, E., Oltramare, C., and de Alencastro, L. F. (2018). Development of a Modified QuEChERS Method for Multi-Class Pesticide Analysis in Human

Hair by GC-MS and UPLC-MS/MS. *Anal. Chim. Acta* 999, 87–98. doi:10.1016/j.aca.2017.11.009

Lippens, B., and Boer, J. H. d. (1965). Studies on Pore Systems in Catalysts V. The T Method. *J. Catal.* 4, 319–323. doi:10.1016/0021-9517(65)90307-6

Liu, L., Li, F.-b., Feng, C.-h., and Li, X.-z. (2009). Microbial Fuel Cell with an Azo-Dye-Feeding Cathode. *Appl. Microbiol. Biotechnol.* 85, 175–183. doi:10.1007/s00253-009-2147-9

Logan, B., Cheng, S., Watson, V., and Estadt, G. (2007). Graphite Fiber Brush Anodes for Increased Power Production in Air-Cathode Microbial Fuel Cells. *Environ. Sci. Technol.* 41, 3341–3346. doi:10.1021/es062644y

Lonappan, L., Rouissi, T., Kaur Brar, S., Verma, M., and Surampalli, R. Y. (2018). An Insight into the Adsorption of Diclofenac on Different Biochars: Mechanisms, Surface Chemistry, and Thermodynamics. *Bioresour. Technol.* 249, 386–394. doi:10.1016/j.biortech.2017.10.039

Lozowicka, B., Kaczyński, P., Szabunko, J., Ignatowicz, K., Warentowicz, D., and Lozowicki, J. (2016). New Rapid Analysis of Two Classes of Pesticides in Food Wastewater by Quechers-Liquid Chromatography/Mass Spectrometry. *J. Ecol. Eng.* 17, 97–105. doi:10.12911/22998993/63478

Maged, A., Dissanayake, P. D., Yang, X., Pathirannahalage, C., Bhatnagar, A., and Ok, Y. S. (2021). New Mechanistic Insight into Rapid Adsorption of Pharmaceuticals from Water Utilizing Activated Biochar. *Environ. Res.* 202, 111693. doi:10.1016/j.envres.2021.111693

Manoli, K., Morrison, L. M., Sumarah, M. W., Nakhla, G., Ray, A. K., and Sharma, V. K. (2019). Pharmaceuticals and Pesticides in Secondary Effluent Wastewater: Identification and Enhanced Removal by Acid-Activated Ferrate(VI). *Water Res.* 148, 272–280. doi:10.1016/j.watres.2018.10.056

Mukhtar, A., Mellon, N., Saqib, S., Lee, S.-P., and Bustam, M. A. (2020). Extension of BET Theory to CO2 Adsorption Isotherms for Ultra-microporosity of Covalent Organic Polymers. *SN Appl. Sci.* 2, 1232. doi:10.1007/s42452-020-2968-9

Musson, S. E., Campo, P., Tolaymat, T., Suidan, M., and Townsend, T. G. (2010). Assessment of the Anaerobic Degradation of Six Active Pharmaceutical Ingredients. *Sci. Total Environ.* 408, 2068–2074. doi:10.1016/j.scitotenv.2009.11.042

Pang, S., Lin, Z., Zhang, W., Mishra, S., Bhatt, P., and Chen, S. (2020). Insights into the Microbial Degradation and Biochemical Mechanisms of Neonicotinoids. *Front. Microbiol.* 11, 868. doi:10.3389/fmicb.2020.00868

Patel, M., Kumar, R., Kishor, K., Mlsna, T., Pittman, C. U., and Mohan, D. (2019). Pharmaceuticals of Emerging Concern in Aquatic Systems: Chemistry, Occurrence, Effects, and Removal Methods. *Chem. Rev.* 119, 3510–3673. doi:10.1021/acs.chemrev.8b00299

Peng, J., Xiao, Y., Cao, H., Zhang, L., and Tang, J. (2013). Determination of Pirimicarb and Paclobutrazol Pesticide Residues in Food by HPLC-ESI-MS with a Novel Sample Preparation Method. *Anal. Lett.* 46, 35–47. doi:10.1080/00032719.2012.708955

Prévoteau, A., Ronsse, F., Cid, I., Boeckx, P., and Rabaey, K. (2016). The Electron Donating Capacity of Biochar Is Dramatically Underestimated. *Sci. Rep.* 6, 32870. doi:10.1038/srep32870

Qin, M., Yang, H., Chen, S., Xie, H., and Guan, J. (2012). Photochemical Characteristics of Diclofenac and its Photodegradation of Inclusion Complexes with β-cyclodextrins. *Quím. Nova* 35, 559–562. doi:10.1590/s0100-40422012000300022

Radovic, L., Moreno-Castilla, C., and Rivera-Utrilla, J. (2000). Carbon Materials as Adsorbents in Aqueous Solutions. *Chem. Phys. Carbon* 27, 247–426. doi:10.1201/9781482270129-11

Rafatullah, M., Sulaiman, O., Hashim, R., and Ahmad, A. (2010). Adsorption of Methylene Blue on Low-Cost Adsorbents: A Review. *J. Hazard. Mater.* 177, 70–80. doi:10.1016/j.jhazmat.2009.12.047

Rejczak, T., and Tuzimski, T. (2015). A Review of Recent Developments and Trends in the QuEChERS Sample Preparation Approach. *Open Chem.* 13, 980–1010. doi:10.1515/chem-2015-0109

Rizzo, L., Fiorentino, A., Grassi, M., Attanasio, D., and Guida, M. (2015). Advanced Treatment of Urban Wastewater by Sand Filtration and Graphene Adsorption for Wastewater Reuse: Effect on a Mixture of Pharmaceuticals and Toxicity. *J. Environ. Chem. Eng.* 3, 122–128. doi:10.1016/j.jece.2014.11.011

Ronsse, F., van Hecke, S., Dickinson, D., and Prins, W. (2013). Production and Characterization of Slow Pyrolysis Biochar: Influence of Feedstock Type and Pyrolysis Conditions. *Gcb Bioenergy* 5, 104–115. doi:10.1111/gcbb.12018

Rouquerol, J., Llewellyn, P., and Rouquerol, F. (2007). Is the BET Equation Applicable to Microporous Adsorbents? *Stud. Surf. Sci. Catal.* 160, 49–56. doi:10.1016/s0167-2991(07)80008-5

Shafiq, M., Alazba, A. A., and Amin, M. T. (2019). Synthesis, Characterization, and Application of Date palm Leaf Waste-Derived Biochar to Remove Cadmium and Hazardous Cationic Dyes from Synthetic Wastewater. *Arab J. Geosci.* 12, 63. doi:10.1007/s12517-018-4186-y

Sharma, A., Kumar, V., Shahzad, B., Tanveer, M., Sidhu, G. P. S., Handa, N., et al. (2019). Worldwide Pesticide Usage and its Impacts on Ecosystem. *SN Appl. Sci.* 1, 1446. doi:10.1007/s42452-019-1485-1

Soloneski, S., and L., M. (2015). "Insecticides - Pest Engineering," in *Chapter 24: Genetic Toxicological Profile of Carbofuran and Pirimicarb Carbamic Insecticides*. Editor F. Perveen (London: Faculty of Natural Sciences and Museum, National University of La Plata Argentina: IntechOpen). doi:10.5772/30137

Stevens-Garmon, J., Drewes, J. E., Khan, S. J., McDonald, J. A., and Dickenson, E. R. V. (2011). Sorption of Emerging Trace Organic Compounds onto Wastewater Sludge Solids. *Water Res.* 45, 3417–3426. doi:10.1016/j.watres.2011.03.056

Tan, X., Liu, Y., Zeng, G., Wang, X., Hu, X., Gu, Y., et al. (2015). Application of Biochar for the Removal of Pollutants from Aqueous Solutions. *Chemosphere* 125, 70–85. doi:10.1016/j.chemosphere.2014.12.058

Tejedor-Sanz, S., Fernández-Labrador, P., Hart, S., Torres, C. I., and Esteve-Núñez, A. (2018). Geobacter Dominates the Inner Layers of a Stratified Biofilm on a Fluidized Anode during Brewery Wastewater Treatment. *Front. Microbiol.* 9, 378. doi:10.3389/fmicb.2018.00378

Tejedor-Sanz, S., Ortiz, J. M., and Esteve-Núñez, A. (2017). Merging Microbial Electrochemical Systems with Electrocoagulation Pretreatment for Achieving a Complete Treatment of Brewery Wastewater. *Chem. Eng. J.* 330, 1068–1074. doi:10.1016/j.cej.2017.08.049

Ternes, T. A., Meisenheimer, M., McDowell, D., Sacher, F., Brauch, H.-J., Haist-Gulde, B., et al. (2002). Removal of Pharmaceuticals during Drinking Water Treatment. *Environ. Sci. Technol.* 36, 3855–3863. doi:10.1021/es015757k

Thommes, M., Kaneko, K., Neimark, A. V., Olivier, J. P., Rodriguez-Reinoso, F., Rouquerol, J., et al. (2015). Physisorption of Gases, with Special Reference to the Evaluation of Surface Area and Pore Size Distribution (IUPAC Technical Report). *Pure Appl. Chem.* 87, 1051–1069. doi:10.1515/pac-2014-1117

Tomczyk, A., Sokołowska, Z., and Boguta, P. (2020). Biochar Physicochemical Properties: Pyrolysis Temperature and Feedstock Kind Effects. *Rev. Environ. Sci. Biotechnol.* 19, 191–215. doi:10.1007/s11157-020-09523-3

Vanreppelen, K., Vanderheyden, S., Kuppens, T., Schreurs, S., Yperman, J., and Carleer, R. (2014). Activated Carbon from Pyrolysis of brewer's Spent Grain: Production and Adsorption Properties. *Waste Manag. Res.* 32, 634–645. doi:10.1177/0734242x14538306

Vergili, I. (2013). Application of Nanofiltration for the Removal of Carbamazepine, Diclofenac and Ibuprofen from Drinking Water Sources. *J. Environ. Manage.* 127, 177–187. doi:10.1016/j.jenvman.2013.04.036

Wang, B., Wang, Z., Jiang, Y., Tan, G., Xu, N., and Xu, Y. (2017). Enhanced Power Generation and Wastewater Treatment in Sustainable Biochar Electrodes Based Bioelectrochemical System. *Bioresour. Technol.* 241, 841–848. doi:10.1016/j.biortech.2017.05.155

Wang, H., Heil, D., Ren, Z. J., and Xu, P. (2015). Removal and Fate of Trace Organic Compounds in Microbial Fuel Cells. *Chemosphere* 125, 94–101. doi:10.1016/j.chemosphere.2014.11.048

Ying, G.-G., and Kookana, R. S. (2004). Simultaneous Determination of Imidacloprid, Thiacloprid, and Thiamethoxam in Soil and Water by High-Performance Liquid Chromatography with Diode-Array Detection. *J. Environ. Sci. Health B Pest Food Contam. Agricul Wastes* 39, 737–746. doi:10.1081/pfc-20003080810.1081/lesb-200030808

Yu, L., Yuan, Y., Tang, J., Wang, Y., and Zhou, S. (2015). Biochar as an Electron Shuttle for Reductive Dechlorination of Pentachlorophenol by Geobacter Sulfurreducens. *Sci. Rep.* 5, 16221. doi:10.1038/srep16221

Yuan, Y., Bolan, N., Prévoteau, A., Vithanage, M., Biswas, J. K., Ok, Y. S., et al. (2017). Applications of Biochar in Redox-Mediated Reactions. *Bioresour. Technol.* 246, 271–281. doi:10.1016/j.biortech.2017.06.154

Żur, J., Marchlewicz, A., Piński, A., Guzik, U., and Wojcieszyńska, D. (2021). Degradation of Diclofenac by New Bacterial Strains and its Influence on the Physiological Status of Cells. *J. Hazard. Mater.* 403, 124000. doi:10.1016/j.jhazmat.2020.124000

Publisher's Note: All claims expressed in this article are solely those of the authors and do not necessarily represent those of their affiliated organizations, or those of the publisher, the editors and the reviewers. Any product that may be evaluated in this article, or claim that may be made by its manufacturer, is not guaranteed or endorsed by the publisher.